AD-A144 016 TEMPORAL EVOLUTION OF WHISTLER GROWTH IN A COLD PLASMA INJECTION EXPERIMENT(U) NAVAL RESEARCH LAB WASHINGTON DC G GANGULI ET AL. 06 JUL 84 NRL-MR-5379 1/1

UNCLASSIFIED F/G 20/9 NL

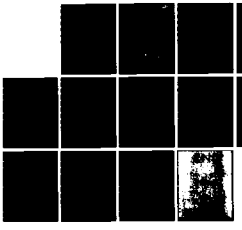

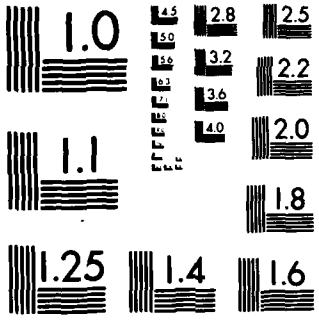

NRL Memorandum Report 5379

Temporal Evolution of Whistler Growth in a Cold Plasma Injection Experiment

G. GANGULI

Science Applications, Inc.
McLean, VA 22102

P. PALMADESSO AND J. FEDDER

Geophysical and Plasma Dynamics Branch
Plasma Physics Division

July 6, 1984

This work was supported by the Office of Naval Research and the National Aeronautics and Space Administration.

NAVAL RESEARCH LABORATORY
Washington, D.C.

SECURITY CLASSIFICATION OF THIS PAGE

REPORT DOCUMENTATION PAGE

1a REPORT SECURITY CLASSIFICATION: UNCLASSIFIED	1b RESTRICTIVE MARKINGS
2a SECURITY CLASSIFICATION AUTHORITY	3 DISTRIBUTION AVAILABILITY OF REPORT: Approved for public release; distribution unlimited.
2b DECLASSIFICATION DOWNGRADING SCHEDULE	
4 PERFORMING ORGANIZATION REPORT NUMBER(S): NRL Memorandum Report 5379	5 MONITORING ORGANIZATION REPORT NUMBER(S)
6a NAME OF PERFORMING ORGANIZATION: Naval Research Laboratory; 6b OFFICE SYMBOL (If applicable): Code 4780	7a NAME OF MONITORING ORGANIZATION
6c ADDRESS (City, State and ZIP Code): Washington, DC 20375	7b ADDRESS (City, State and ZIP Code)
8a NAME OF FUNDING/SPONSORING ORGANIZATION: ONR and NASA; 8b OFFICE SYMBOL (If applicable)	9 PROCUREMENT INSTRUMENT IDENTIFICATION NUMBER
8c ADDRESS (City, State and ZIP Code): Arlington, VA 22217 Washington, DC 20546	10 SOURCE OF FUNDING NOS: PROGRAM ELEMENT NO 61153N; PROJECT NO RR033-02-44; TASK NO W-14365; WORK UNIT NO DN880-025
11 TITLE (Include Security Classification): (See page ii)	
12 PERSONAL AUTHOR(S): Ganguli, G.,* Palmadesso, P., and Fedder, J.	
13a TYPE OF REPORT: Interim; 13b TIME COVERED: FROM 10/83 TO 10/84; 14 DATE OF REPORT (Yr., Mo., Day): July 6, 1984; 15 PAGE COUNT: 30	
16 SUPPLEMENTARY NOTATION: *Science Applications, Inc., McLean, VA 22102 (Continues)	
17 COSATI CODES: FIELD / GROUP / SUB GR	18 SUBJECT TERMS (Continue on reverse if necessary and identify by block number): Artificial aurora; Particle precipitation; AMPTE

19 ABSTRACT (Continue on reverse if necessary and identify by block number)

Using a simple time dependent cold plasma density model and assuming a typical ambient radiation belt environment, we study the evolution of the whistler mode turbulence and particle precipitation in a cold plasma release experiment similar to one which may be conducted as part of the AMPTE program. It is known from earlier work that the release of cold lithium ions can significantly lower the critical energy E_c above which the resonant radiation belt electrons can pitch angle scatter. We study the time evolution of the one pass gain factor for a whistler wave packet and find that for parameters accessible to AMPTE type experiments the gain factor is large enough to ensure strong whistler turbulence and strong pitch angle diffusion of radiation belt particles with energies in the range between the ambient value of E_c and the reduced value of E_c. Estimates for the total power input to the ionospheric footprint of the release are of the order of an erg/cm^2/sec. This precipitated energy should produce a patch of visible aurora. This effect should also persist for many hours.

20 DISTRIBUTION/AVAILABILITY OF ABSTRACT: UNCLASSIFIED/UNLIMITED X SAME AS RPT DTIC USERS	21 ABSTRACT SECURITY CLASSIFICATION: UNCLASSIFIED
22a NAME OF RESPONSIBLE INDIVIDUAL: P. Palmadesso	22b TELEPHONE NUMBER (Include Area Code): (202) 767-6780
	22c OFFICE SYMBOL: Code 4700.1P

DD FORM 1473 83 APR EDITION OF 1 JAN 73 IS OBSOLETE

SECURITY CLASSIFICATION OF THIS PAGE

11. TITLE (Include Security Classification)

Temporal Evolution of Whistler Growth in a Cold Plasma Injection Experiment

16. SUPPLEMENTARY NOTATION (Continued)

This work was supported by the Office of Naval Research and the National Aeronautics and Space Administration.

CONTENTS

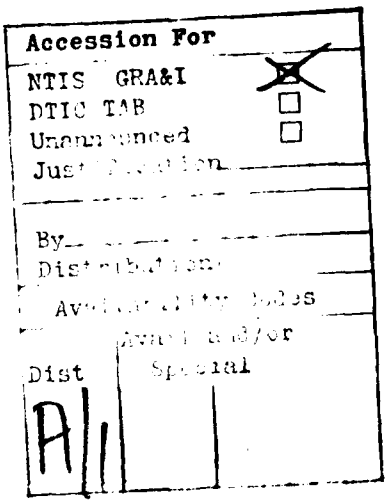

TEMPORAL EVOLUTION OF WHISTLER GROWTH IN A COLD PLASMA INJECTION EXPERIMENT

Introduction

Energetic electron precipitation has been of considerable interest for over two decades. Bursts of precipitation were observed by balloon x-ray bremsstrahlung measurements as early as 1963 [Winckler et al., 1963; Anderson and Milton, 1964] and in-situ measurements of greater than 40-keV electron fluxes were made by Injun 3 [O'Brien, 1964]. The importance of loss cone electromagnetic cyclotron (EMC) instabilities in the magnetosphere and the relevance of such instabilities to particle precipitation processes was first pointed out by Cornwall (1965), and independently, by Obayashi (1965). An attempt to formulate a theory of particle trapping and precipitation under the influence of EMC instabilities was made by Kennel and Petschek (1966). Kennel and Petschek studied the wave growth and loss rates of whistler, ion-cyclotron and magnetosonic waves in a finite plasma (i.e., magnetosphere) and derived a limit on the stably trapped particle fluxes in the radiation belts. Subsequently, more rigorous and self-consistent studies of these processes have been conducted, with the result that some of the conclusions of Kennel and Petschek must be modified (Etcheto et al., 1973). Cocke and Cornwall (1967) suggested that cold plasma played an important role in controlling the wave particle interactions in the radiation belts within the plasmasphere. Later Brice [1969] pointed out that cold plasma injected from the ionosphere into the magnetosphere could produce enhanced whistler-mode turbulence and associated precipitation of energetic electrons, while Cornwall et al. [1970] recognized a parallel process for the ion cyclotron waves and ion precipitation.

Brice [1970], and Brice and Lucas [1971], have suggested that a substantial increase in the energetic electron precipitation could be

Manuscript approved May 7, 1984.

achieved by injection of very modest amounts of cold plasma into the radiation belts. A hypothetical experiment in which VLF EMC noise and proton precipitation could be enhanced by lithium injection was analyzed by Cornwall (1974). Similarly, enhancement of VLF EMC noise and electron precipitation by barium injection was studied by Liemohn (1974).

Under certain conditions the injection can introduce a new limit to the number of stably trapped particles [Kennel and Petschek, 1966]. Electrons with energies below a certain threshold energy E_c will continue to be trapped and those with energies higher than E_c may be precipitated provided conditions regarding their degree of anisotropy and relative abundance are satisfied. For ambient cold plasma densities the threshold energy E_{c1} is greater than the thermal energy of the hot particles, and the energetic electron density can increase to a large value. With the injection of additional cold plasma, the threshold energy is reduced from E_{c1} to E_{c2} and electrons with energies between E_{c1} and E_{c2} create growing waves, are pitch angle scattered and precipitate into the atmosphere. This precipitation may produce an artificial aurora which is observable from the ground.

Cuperman and Landau [1976] have studied the theory of the electromagnetic electron cyclotron (whistler) instability produced by addition of cold plasma to an infinite uniform anisotropic plasma. Their formalism disregards the finite size of the region of cold plasma enhancement in the magnetosphere and uses a stationary model for the cold plasma density. We extend the Cuperman and Landau model to study a time varying cold plasma density injection $n_c(t)$; and take into account the finite size of the flux tube by studying the wave gain as a function of both the spatial and the temporal growth rates of the waves.

The purpose of this brief report is to make semi-quantitative estimates of the magnitude and the duration of the enhancement of VLF EMC noise and electron precipitation effects which might be produced by a cold lithium release experiment in the parameter range accessible to AMPTE.

Model

We assume a point injection of neutral lithium gas. The neutral lithium has a Maxwellian distribution and is allowed to expand radially into the vacuum. Solar radiation ionizes the expanding lithium gas with a time scale of 3000 seconds. After ionization the cold plasma is frozen to the geomagnetic field and its volume increases in time as a geomagnetic field-aligned cylinder (see fig. 1). The cylinder has a radius R_0 and its length is a function of time L(t), so that its volume is $\pi R_0^2 L(t)$.

To estimate the number of cold lithium ions in this field aligned cylinder we also modeled the evolution of the neutral lithium injection cloud. We assume a release of 100 Kg of neutral lithium and a yield of 6% so that the total number of vaporized lithium atoms is $\sim 1.2 \times 10^{26}$. The initial distribution of neutral atoms injected at a point R_1 has a distribution

$$f_0(\underline{v}, \underline{R}, 0) = \frac{N_0}{(\pi v_0)^{3/2}} \delta(R-R_1) \exp\{- v^2/v_0^2\} \qquad (1)$$

with thermal velocity $v_0 \sim 4.5$ km/sec.

Integrating over the initial distribution gives the neutral lithium density as a function of radius from the release point and time

$$n_0(\underline{R}, \underline{t}) = e^{-t/\tau_i} \iiint f_0(\underline{v}, \underline{R} - \underline{v}t, 0)d^3v, \tag{2}$$

where τ_i is the ionization time for neutral lithium atoms. Initially we are interested only in the total number of ions in the flux tube and not their position in the tube, so we have neglected transport of ionized lithium. The rate at which lithium ions are created is given by

$$\frac{d}{dt} n_i(R, t) = \frac{1}{\tau_i} n_0(R, t). \tag{3}$$

Assuming a finite extent of the whistler wave packet across the magnetic field of $R_0 \sim O(\lambda_\perp)(\sim 50$ kms) we integrate (3) from 0 to R_0 and in time from 0 to ∞ to estimate the total number of lithium ions deposited within a sphere of radius R_0 ($N_i \sim 5 \times 10^{23}$ cm^{-3}) which becomes a field aligned flux tube since the ions are trapped by the magnetic field. The actual rate of appearance of the lithium ions in the flux tube is $N_i(1 - e^{-t/\tau_i})$. Additional ions are created outside the flux tube which have much lower density and are not accounted for in this estimate. Estimating the effects of ion transport we find that the cylindrical length L(t) increases linearly in time at a velocity v_0 in both directions along the flux tube. Thus the time dependent model for the cold ion density is given by

$$n_c(t) = \frac{N_i}{(2V_0 t)(\pi R_o^2)} (1 - e^{-t/\tau_i})$$

$$= 12.8 \times 10^8 (R_0/L_0)(\frac{1 - e^{-T}}{T}) \text{ per meter}^3, \tag{5}$$

where $L_0 = 2V_0\tau_i$ and $T = t/\tau_i$. This density is somewhat higher than the average flux tube density because the neutral and ionized lithium is peaked at the center of the flux tube. Figure (2) shows the decay of the cold lithium density as a function of the normalized time T. However, the ionized lithium also is magnetically trapped along the field lines by the mirror force. The condition for the low-energy lithium ions to be mirrored above the ionosphere after being released at the equator in the altitude range of 5 to 8 r_e is $\frac{1}{2} m v_{\perp 0}^2 \gtrsim 0.02$ ev (see Appendix). Since the thermal energy is much greater than 0.02 ev the majority of the lithium ions will remain trapped at high altitudes in the magnetosphere and will be unable to leak into the ionosphere. This will ensure a saturation of the cold lithium ions for large T at a value larger than the lowest value shown in figure (2). Based on the presence of magnetic trapping we expect the cold density will saturate around $T \sim 2$ at a value of around 1.0 cm^{-3}.

We now discuss the critical resonance energy criterion in the presence of a time dependent cold plasma density. It is well known that wave particle interaction can occur when the resonance energy E_R is greater than or equal to the threshold energy E_c. E_R was defined by Kennel and Petschek [1966] as

$$E_R = \frac{1}{2} m V_R^2, \tag{6}$$

where $V_R = \frac{\omega - \Omega}{k_\parallel}$ is the resonance velocity. Taking into account the dispersion relation for the wave, Cornwall [1972] calculated a minimum energy condition for resonance given by

$$E > E_c = \frac{B^2}{8\pi N} A_c^{-1}(1 + A_c)^{-2}, \tag{7}$$

where $A_c \equiv (\Omega_e/\omega - 1)^{-1}$. Using the dispersion relation as given in Cuperman [1974] we can write

$$A_c = \frac{a^2}{\alpha(t)\beta}, \tag{8}$$

where $a = k\rho$, $\rho = v_{th}/\Omega_e$, $\alpha = 1 + n_c(t)/n_w$ is the energetic electron density and $\beta = n_w KT/(B^2/8\pi)$, where K is the Boltzman constant and the subscript w refers to the warm electron component. Thus we can rewrite (7) as

$$\frac{E_c}{E_{th}} = \frac{1}{\alpha(t)\beta A(1 + A)^2}, \tag{9}$$

where E_{th} is the thermal energy of the energetic electrons.

In the absence of cold plasma $\alpha = 1$ and E_c is a constant. This is indicated in Fig. (3) top line. Here we took the density of the ambient electrons to be 0.5 per cubic centimeter, their thermal energy $E_{th} \sim 2.0$ keV, a magnetic field of 10^{-3} gauss, the degree of anisotropy $A \sim 0.50$ and $\beta \sim 0.07$. With the addition of cold plasma E_c is sharply reduced especially at early times, thereby enabling a very large population of energetic electrons to interact with the waves, enhancing the whistler mode turbulence, and thus as a consequence of pitch angle scattering precipitate electrons into the atmosphere. Although E_c does increase somewhat at later times it is still much lower than in the absence of the injected cold plasma. Further, as described earlier, magnetic trapping of the cold lithium ions will not allow the cold plasma density to fall as rapidly as indicated in Fig. (2), thereby ensuring a low E_c for a considerable length of time.

Results

In the previous section we saw that the introduction of the cold plasma considerably lowers the threshold energy and thus enhances the growth of whistler noise turbulence. Since the flux tube where the cold plasma is enhancing wave particle interaction has a finite length, the temporal growth rate alone cannot determine the extent of the wave growth because the waves propagate away from the region of rapid growth. Therefore we consider the spatial growth rates and finally calculate the net gain G, of the wave during a single pass through the flux tube. The condition for a large effect is GR >1 where R is the reflection coeffic t for the wave at the ionosphere. The waves with ln G >> 1, a more s re condition, will experience a significant gain in the wave amp de independent of R, leading to strong whistler turbulence and considerable pitch angle scattering of the electrons interacting with the waves. The gain G of the wave is defined as

$$G = e^{g}, \tag{10}$$

$$g = \begin{cases} \dfrac{\gamma(\omega,k)L(t)}{V_g(\omega,k)} & , \quad L(t) < 4r_e \\ 4\,\dfrac{\gamma}{V_g}\,r_e & , \quad L(t) > 4r_e, \end{cases} \tag{11}$$

where $\gamma(\omega,k)$ is the temporal growth rate of the whistler mode instability, $V_g = \partial\omega_r/\partial k$, is the group velocity of the whistler mode and r_e is one earth radius. Since the whistler mode is excited primarily in the equatorial region where the magnetic field is nearly uniform and straight, we have limited the length L(t) in (11) to $4r_e$.

In order to evaluate $\gamma(\omega,k)$ and $V_g(\omega,k)$ for the resonant energy we solve the expression (32) of Cuperman and Landau [1974]

$$\frac{a^2}{\alpha\beta} = \frac{\bar{\omega}}{1 - \bar{\omega}}, \quad \bar{\omega} = \omega/\Omega_e, \tag{12}$$

and the resonance condition

$$\bar{\omega} = 1 + a\,\bar{v}_R, \quad \bar{v}_R = \frac{v_R}{v_{th}}, \tag{13}$$

simultaneously. Eliminating $\bar{\omega}$ from (12) and (13) we obtain a cubic equation for 'a' given by

$$a^3 + \alpha\beta a + \frac{\alpha\beta}{\bar{v}_R} = 0. \tag{14}$$

We solve (14) using a numerical root finder for 'a'. Then 'a' is used to evaluate the group velocity V_g from (12) and the temporal growth rate γ/Ω_e from the expression (33) of Cuperman and Landau [1974]. With these quantities g is evaluated for the resonant waves.

The observed differential flux for radiation belt electrons is not a Maxwellian for energies higher than 30 keV which is a typical E_c for ambient cold plasma distribution between 5 and 8 r_e. The observed flux is given by a power law of the form

$$j = C_1 E^{-J} \text{ electrons/cm}^2 \text{ STER. sec. keV}, \tag{15}$$

which corresponds to the energy distribution function given by

$$f(E) = C_\sigma E^{-(1 + \sigma)}. \qquad (16)$$

We have considered two distributions of the following form for the energetic electrons corresponding to quiet and disturbed magnetospheric conditions respectively;

$$f_w = n_w\left(\frac{m_e}{2\pi kT}\right)^{3/2} \exp\left(- E/E_{th}\right) + C_\sigma E^{-(1 + \sigma)}; \qquad (17)$$

where σ is either 3/2 or 3 and $C_{3/2} = 4.72 \times 10^{51}$, $C_3 = 6.7 \times 10^{54}$ (private communication, D. Williams, 1983). We note that the power law applies only for particle energies in excess of 30 keV which is a typical value for E_c. Above E_c the stable flux is limited as shown by Kennel and Petschek [1966] and others. Below E_c the ambient flux is not limited by the wave processes and can therefore be larger. For ease of calculation we make a conservative estimate of the flux in this energy range by extending the power law to lower energies.

Figure (4) is a plot of g(T) which is ln G(T), as a function of T for $\sigma = 3/2$ for characteristic particle energies spanning from 20 to 40 keV in steps of 5 keV. We chose plasma parameters such that A = 0.75, $\beta = 0.07$, $E_{th} = 2$ keV and the density of energetic electrons $n_w = 0.5$ per cc. The gain curves rapidly increase until the injected electrons fill a flux tube of length $4r_e$ and thereafter show a very mild decrease due to the decrease in the temporal growth rate. The group velocity shows very little variation with time.

Figure (5) is a plot similar to Figure (4) except here $\sigma = 3$. The overall behavior of both figures (4) and (5) are similar.

Figure (6) is a plot of g against time for a typical energetic particle energy of 30 keV for various values of β. It shows that the wave gain is quite sensitive to the value of β. For higher β the gain increases. Therefore if magnetic fluctuations are taken into account β will fluctuate and with it the wave gain.

Overall, we find a significant wave gain for a single pass through the flux tube especially for lower energy particles. Nevertheless, at 25 keV the gain factor is already large enough to ensure strong turbulence and strong pitch angle diffusion. For lower energies the gain factor becomes too large for the linear theory to be meaningful; this indicates that non linear processes (i.e. strong pitch angle scattering) are important at these energies. Figure 7 shows a gain versus time plot for lower energies (4 to 12 keV). The gain g(T) increases to a very large number as the energy decreases until the particle energy is around 8 to 10 keV, while for still lower energies the gain is reduced. This decrease occurs for particle energy near E_c.

Conclusion

Using a simple time dependent cold plasma density model we have shown that a cold lithium injection in the AMPTE parameter range can give rise to whistler mode turbulence with significant gain to the wave amplitude in a single pass through the flux tube. Whistler mode growth gives rise to pitch angle diffusion of the energetic electrons which then precipitate. As energetic electrons are removed by precipitation new electrons drift into the flux tube via gradient and curvature drift motion. An equilibrium

can be established in which newly supplied radiation belt electrons in excess of the new stable trapping limit are continuously precipitated. The rate of power input into the ionosphere can thus be estimated roughly as follows:

$$\frac{\text{Power Input to Flux Tube}}{\text{Area of Ionospheric Foot}} = n_{\omega}^{eff}\, kT^{eff} V_{drift} \frac{A_{side}}{A_{foot}} . \qquad (18)$$

In (18), the ionospheric crossection of the flux tube, $A_{foot} \sim (\pi R_o^2) B_M / B_I$, ($B_I$ and B_M are the magnetic fields in the ionosphere and the magnetosphere) and the meridianal crossection of the flux tube, $A_{side} \sim R_o L(t)$ give a typical value for the ratio $A_{side}/A_{foot} \sim 5 \times 10^4$. Using a reasonable distribution for the energetic electrons we estimate $n_{\omega}^{eff} \sim 10^{-2} cm^{-3}$. Very large wave gain occurs for particles of energy 10 keV which have $KT^{eff} \sim 10^{-9}$ ergs and a $V_{drift} \sim 5 \times 10^5 cm^{-2} sec^{-1}$. Using these numbers in (18) we find a precipitated power of 2 ergs cm^{-2} sec^{-1}. This value of the precipitated power is large enough to produce a visible aurora. The precipitation would be expected to continue producing a visible aurora until the injected cold plasma in the flux tube is lost or destroyed by magnetospheric convection or other processes.

Acknowledgments

The authors would like to acknowledge important discussions with Dr. D. Williams and Dr. S.M. Krimigis. This work was supported by the Office of Naval Research and the National Aeronautics and Space Administration.

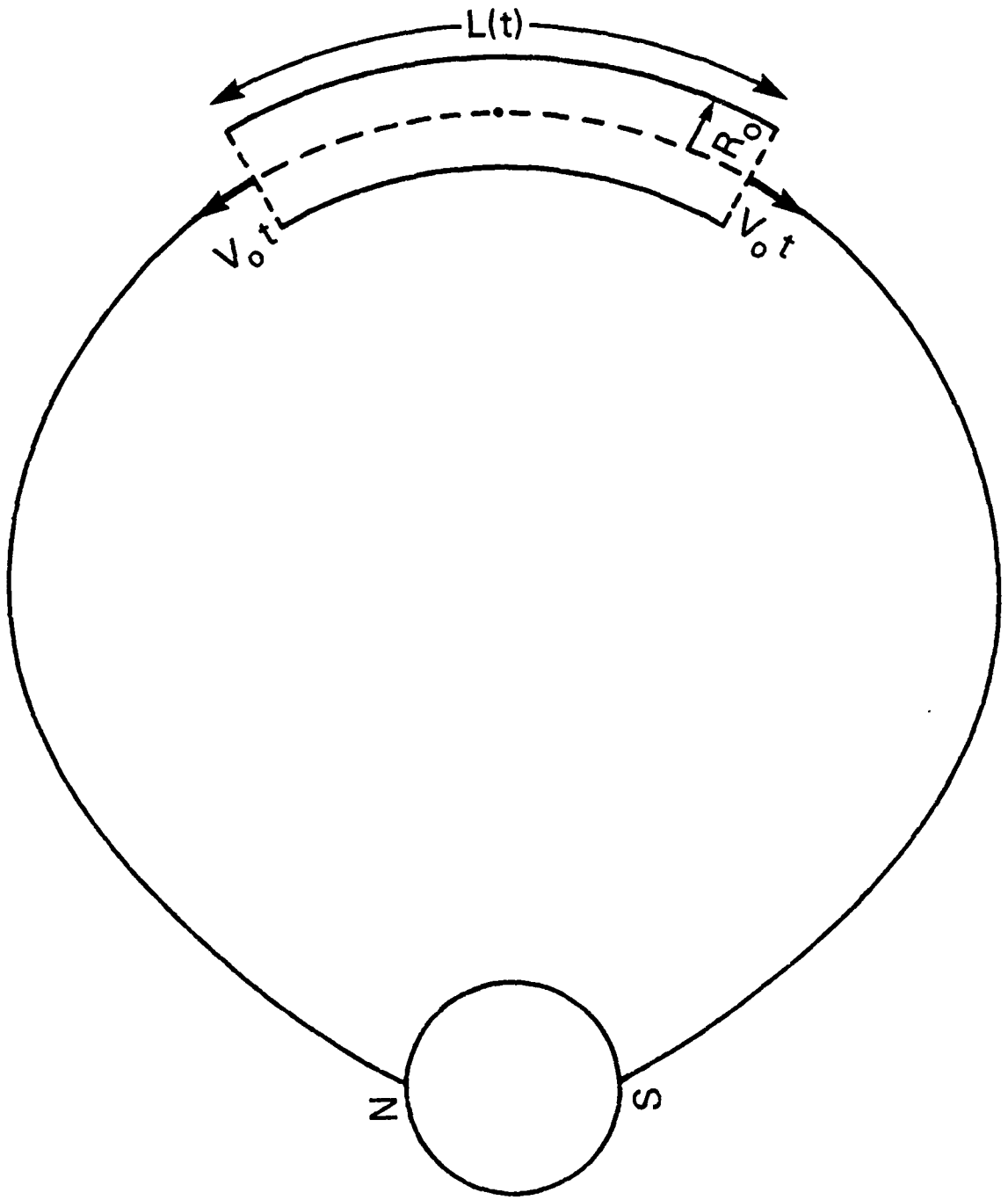

Fig. (1) A schematic representation of the cylindrical cold plasma volume.

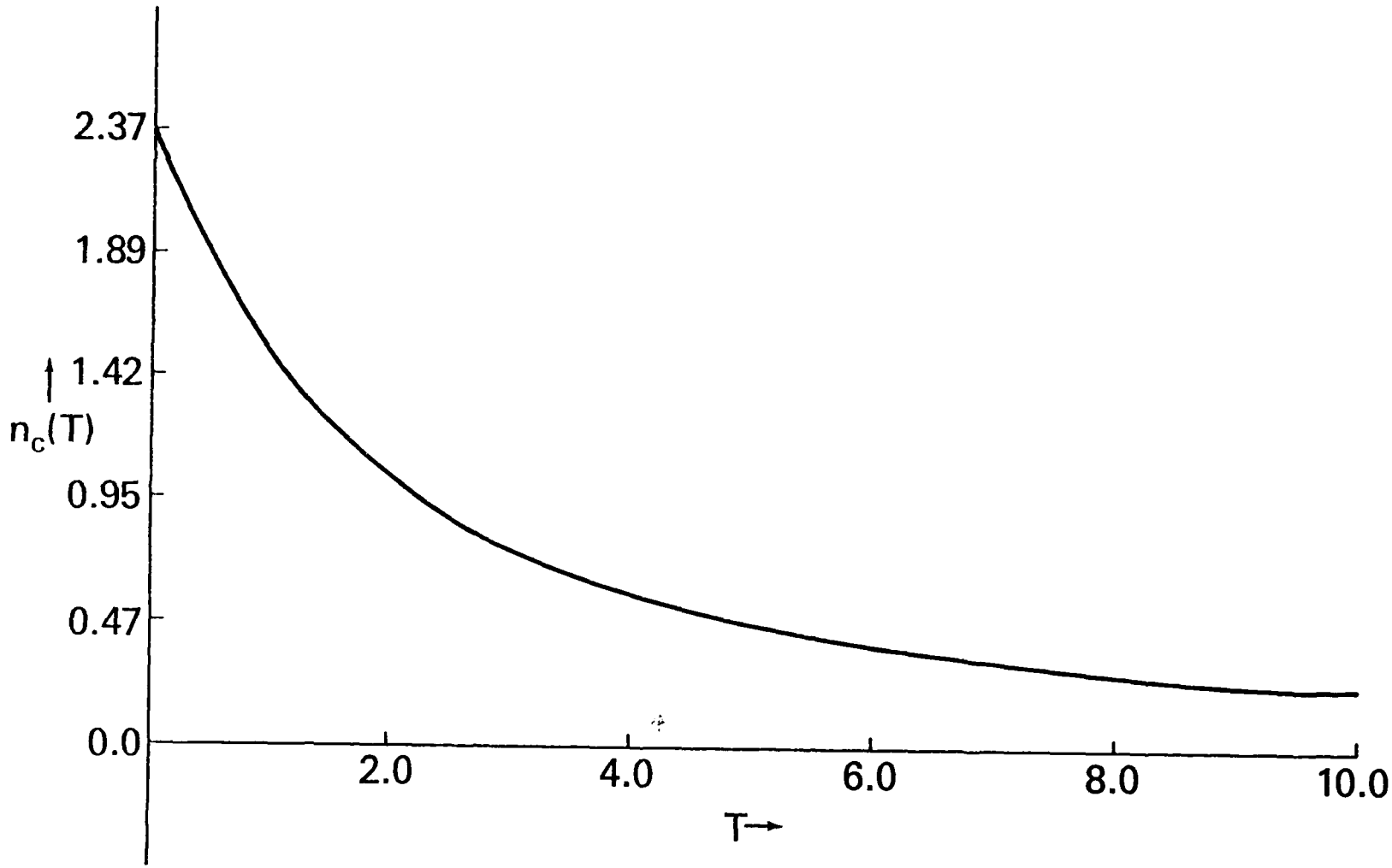

Fig. (2) A plot of $n_c(T)$ against T.

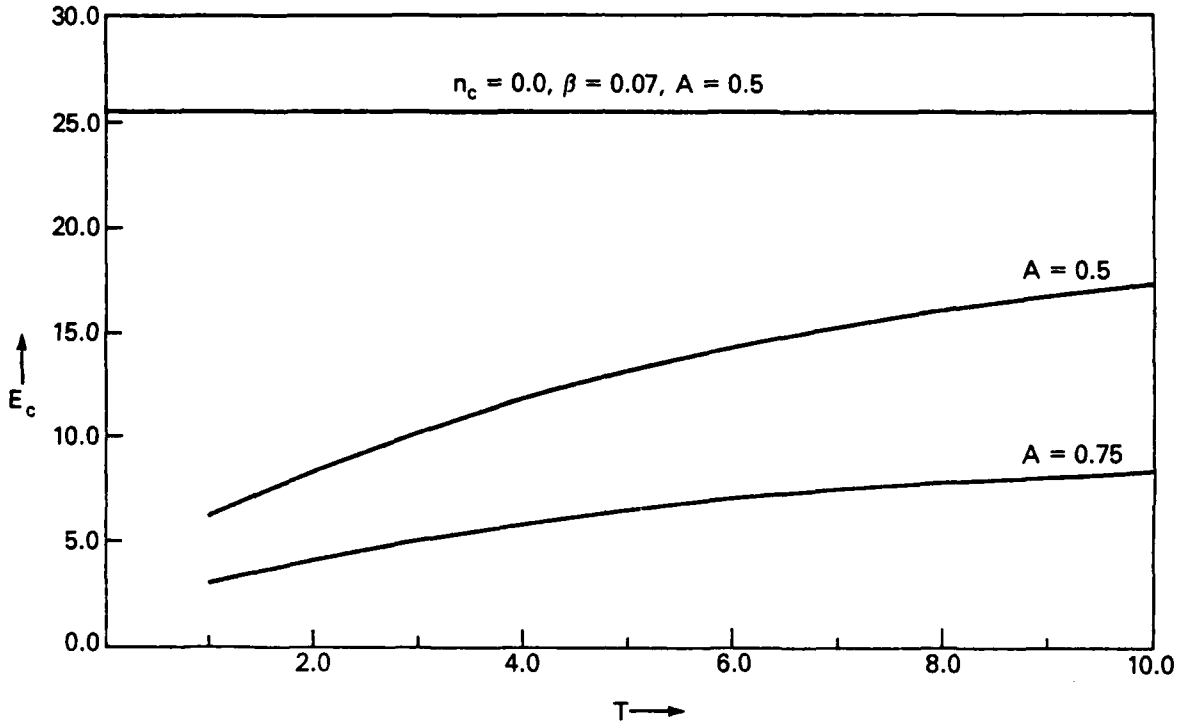

Fig. (3) A plot of the ratio of the critical energy to the background warm electron energy, E_c, against T. The top line corresponds to n_c = 0, β = 0.07 and A = 0.5. The lower curves are for A = 0.5 and 0.75, with β = 0.07 and $n_e(T)$.

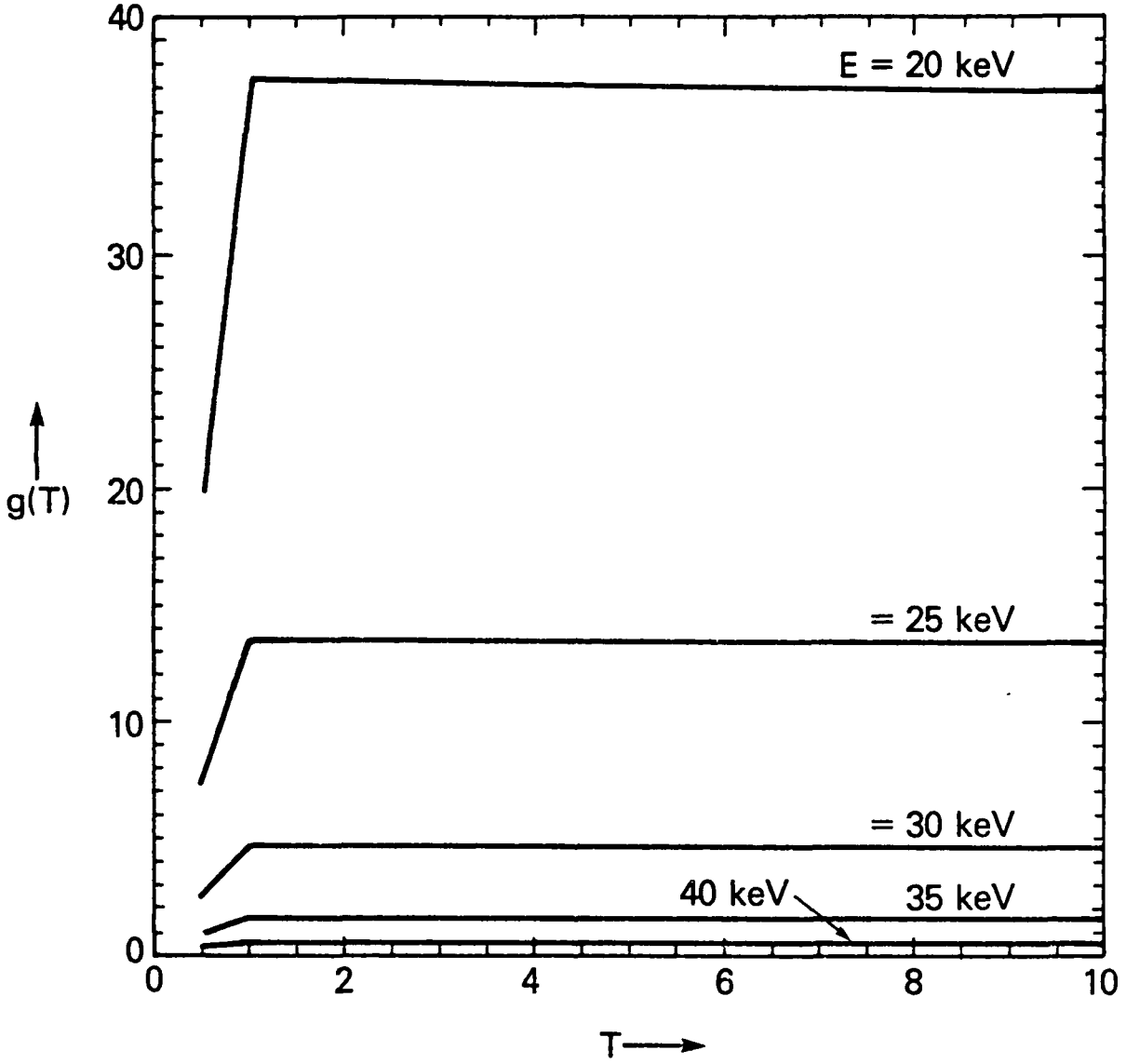

Fig. (4) A plot of g(T) against T for $\sigma = 3/2$ for typical particle energy varying from 20 to 40 keV. Here A = 0.75, $\beta = 0.07$, $n_{\omega} = 0.5$/cc and E_{th} for the electrons is 2 keV.

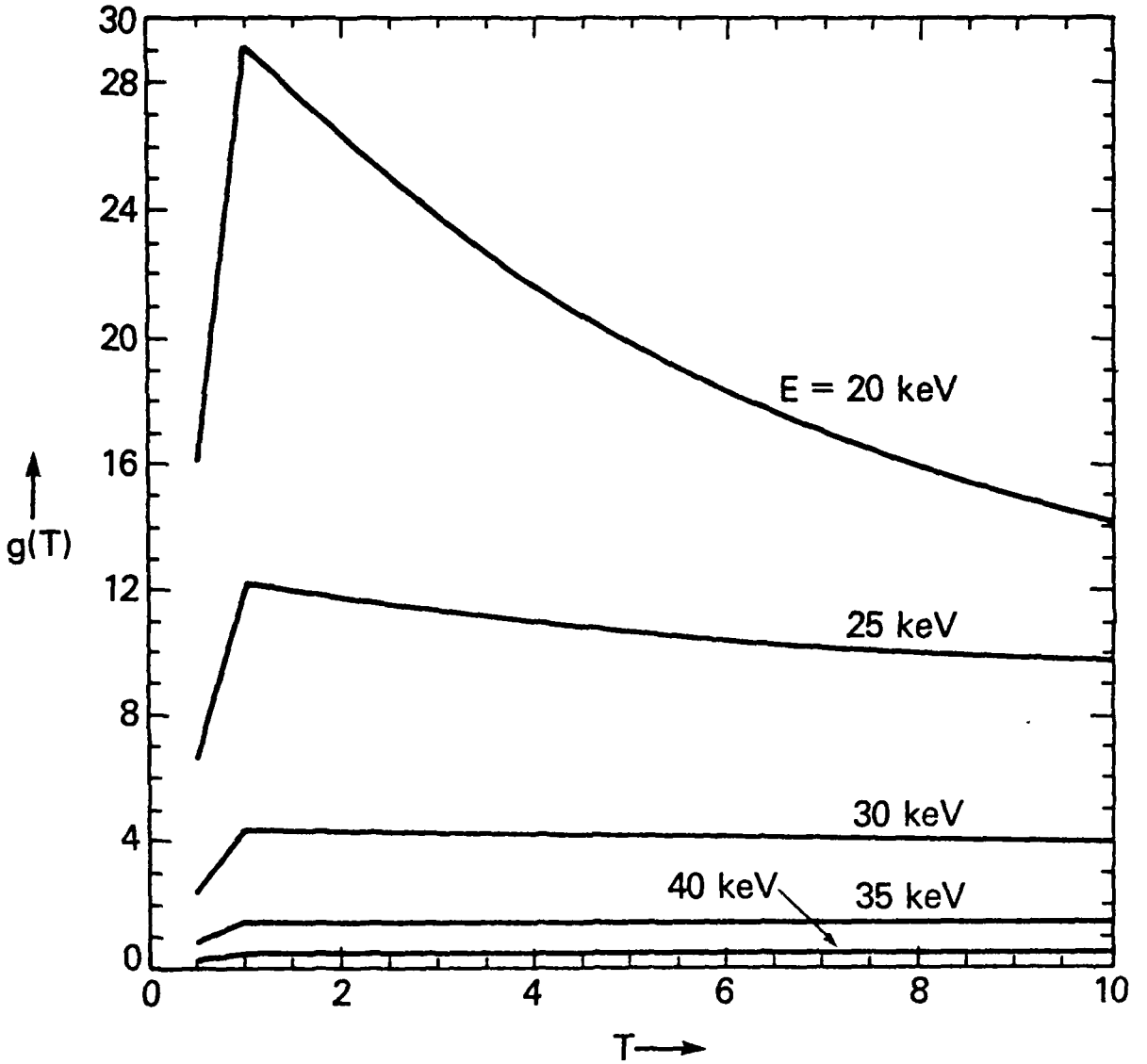

Fig. (5) A plot similar to Fig. (4) but with $\sigma = 3$.

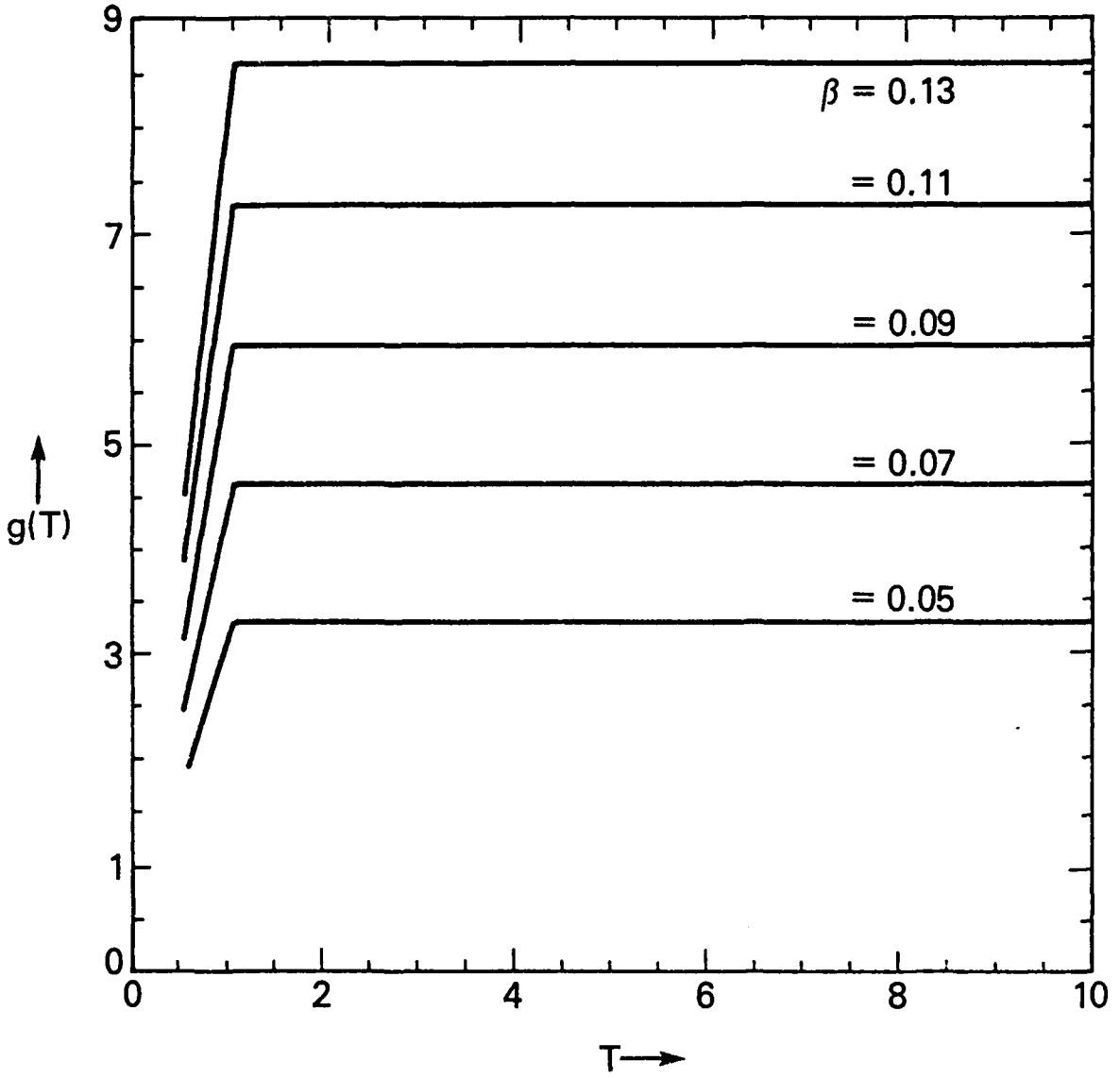

Fig. (6) A plot similar to Fig. (4). Here the typical particle energy is 30 keV. We vary the value of β from 0.05 to 0.13 to demonstrate the sensitivity of g(T) on β. Rest of the parameters are identical to Fig. (4).

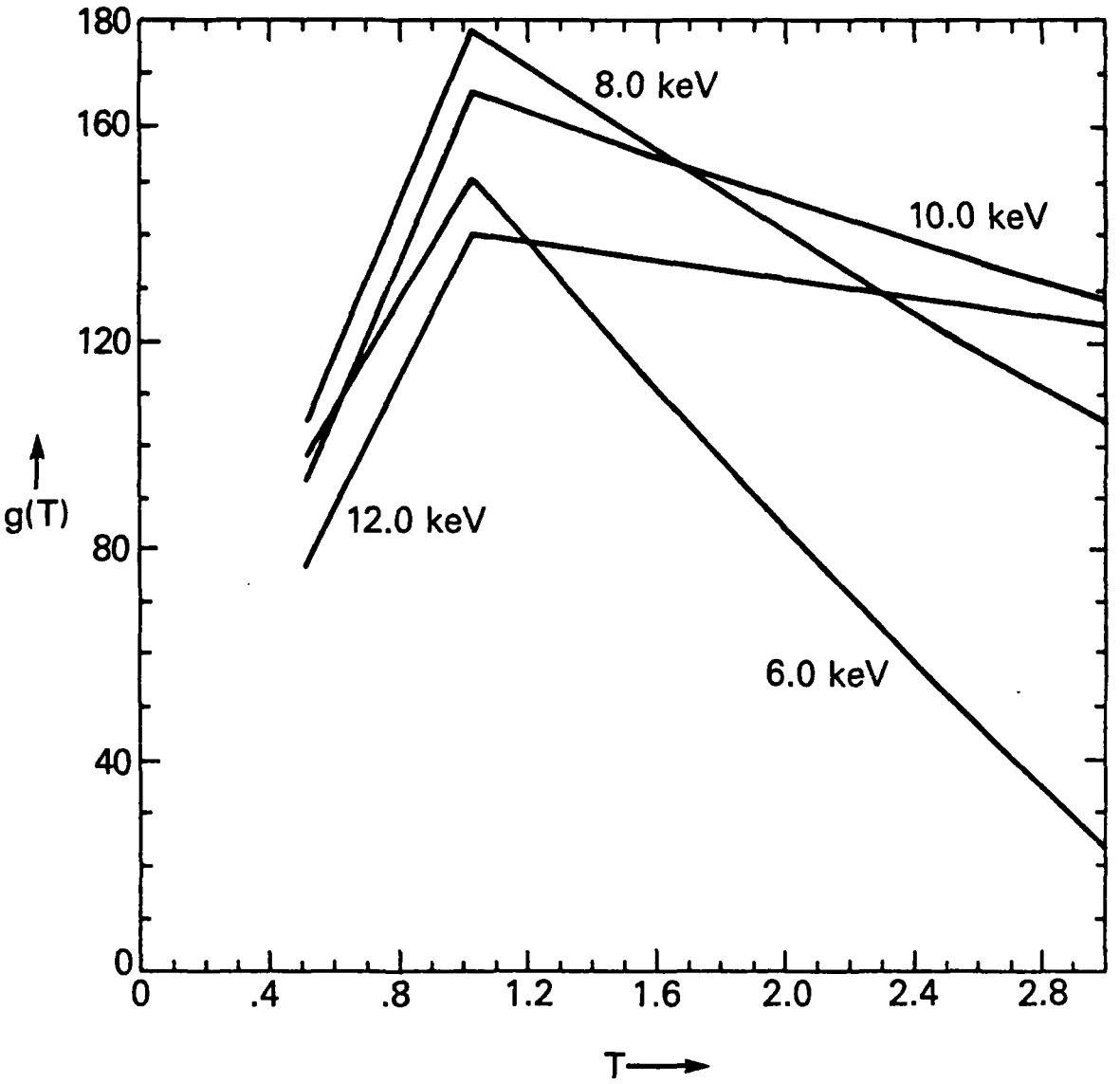

Fig. (7) A plot of g(T) against T for lower energies.

Appendix

Here we calculate the minimum perpendicular energy for lithium ions in the magnetosphere to be trapped at high altitude by the magnetic mirror force. The total energy of the lithium ions is given by

$$E = \frac{1}{2} m v_{\parallel}^2 + \mu B - \frac{G Mm}{r} , \tag{A1}$$

where $\mu = \frac{1}{2} m v_{\perp}^2 / B$, and G is the gravitational constant. Requiring conservation of energy, the net energy in the magnetosphere must be equal to the net energy in the ionosphere,

$$E_M = E_I . \tag{A2}$$

In order to be magnetically trapped in the magnetosphere the ions must have $v_{\parallel I} = 0$. Thus

$$\frac{1}{2} m v_{\perp M}^2 \gtrsim \frac{- G Mm\left[\frac{1}{r_I} - \frac{1}{r_M}\right] - \frac{1}{2} m V_{\parallel M}^2}{1 - \frac{B_I}{B_M}} . \tag{A3}$$

Taking 6 ev for the net gravitational energy, 0.5 ev for the parallel thermal energy in the magnetosphere and $1 - B_I/B_M \sim 287$, we find,

$$\frac{1}{2} m V_{\perp M}^2 \gtrsim 0.02 \text{ ev},$$

for trapping to occur.

References

(1) Anderson, K.A., and D.W. Milton, Balloon observations of X-rays in the auroral zone, 3, High time resolution studies, J. Geophys. Res., 69(21), 1964. p. 4457

(2) Brice, N.M., Artificial Enhancement of Energetic Particle Precipitation through Cold Plasma Injection: A technique for seeding substorms?, J. Geophys. Res., 75(25), p. 4890 1970. Brice, N. and C. Lucas, Influence of magnetospheric convection and polar wind loss of electrons from the outer radiation belt, J. Geophys. Res., 76(4), 900, 1971.

(3) Cocke, W.J., and J.M. Cornwall, Theoretical Simulation of Micropulsations, J. Geophys. Res., 72, 2843, 1967.

(4) Cornwall, J.M., Cyclotron Instabilities and Electromagnetic Emission in the Ultra Low Frequency and Very Low Frequency Ranges, J. Geophys. Res., 70, 61, 1965.

(5) Cornwall, J.M., Magnetosphere Dynamics with Artificial Plasma Clouds, Space Sci. Rev., 15, 841, 1974.

(6) Cornwall, J.M., Precipitation of auroral and ring current particles by artificial plasma injection, Rev. Geophys. Space Phys., 10, 993, 1972. Cornwall, J.M., F.V. Coroniti, and R.M. Thorne, Turbulent loss of ring current protons (abstract), EOS, Trans. AGU, 51, 378, 1970.

(7) Cuperman, S., and R.W. Landau, On the enhancement of the whistler mode instability in the magnetosphere by cold plasma injection, J. Geophys. Res., 79(1), 128, 1976.

(8) Etcheto, J., R. Gendrin, J. Solomon, and A. Roux, A Self-Consistent Theory of Magnetospheric ELF Hiss, J. Geophys. Res., 78, 8150, 1973.

(9) Kennel, C.F., and H.E. Petschek, Limit on stably trapped particle fluxes, J. Geophys. Res., 71(1), 1, 1966.

(10) Liemohn, H.B., Simulation of VLF Amplification in the Magnetosphere, Space Sci. Rev., 15, 861, 1974.

(11) Obayashi, T., Hydromagnetic Whistlers, J. Geophys. Res., 70, 1069, 1965.

(12) O'Brien, B.J., High-latitude geophysical studies with satellite Injun 3, 3. Precipitation of electrons into the atmosphere, J. Geophys. Res., 69(1), 13, 1964.

(13) Winckler, J.R., P.D. Bhavsar, and K.A. Anderson, A study of the precipitation of energetic electrons from the geomagnetic field during magnetic storms, J. Geophys. Res., 67, 3717, 1962.

DISTRIBUTION LIST

Director
Naval Research Laboratory
Washington, D.C. 20375
ATTN: Code 4700 (26 Copies)
Code 4701
Code 4780 (100 copies)
Code 4187 (E. Szuszczewicz)
Code 4187 (P. Rodriguez)

University of Alaska
Geophysical Institute
Fairbanks, Alaska 99701
ATTN: Library
S. Akasofu
J. Kan
J. Roederer
L. Lee

University of Arizona
Dept. of Planetary Sciences
Tucson, Arizona 85721
ATTN: J.R. Jokipii

University of California, S.D.
LaJolla, California 92037
(Physics Dept.):
ATTN: J.A. Fejer
T. O'Neil
J. Winfrey
Library
J. Malmberg
(Dept. of Applied Sciences):
ATTN: H. Booker

University of California
Los Angeles, California 90024
(Physic Dept.):
ATTN: J.M. Dawson
B. Fried
J.G. Moralles
W. Gekelman
R. Stenzel
Y. Lee
A. Wong
F. Chen
M. Ashour-Abdalla
Library
J.M. Cornwall

(Institute of Geophysics and
Planetary Physics):
ATTN: Library
C. Kennel
F. Coroniti

Columbia University
New York, New York 10027
ATTN: R. Taussig
R.A. Gross

University of California
Berkeley, California 94720
(Space Sciences Laboratory):
ATTN: Library
M. Hudson
(Physics Dept.):
ATTN: Library
A. Kaufman
C. McKee
(Electrical Engineering Dept.):
ATTN: C.K. Birdsall

University of California
Physics Department
Irvine, California 92664
ATTN: Library
G. Benford
N. Rostoker
C. Robertson
N. Rynn

California Institute of Technology
Pasadena, California 91109
ATTN: R. Gould
L. Davis, Jr.
P. Coleman

University of Chicago
Encrico Fermi Institute
Chicago, Illinois 60637
ATTN: E.N. Parker
I. Lerche
Library

Thayer School of Engineering
Dartmouth College
Hanover, NH 03755
ATTN: Bengt U.O. Sonnerup

University of Colorado
Dept. of Astro-Geophysics
Boulder, Colorado 80302
ATTN: M. Goldman
Library

Cornell University
School of Applied and Engineering Physics
College of Engineering
Ithaca, New York 14853
ATTN: Library
R. Sudan
B. Kusse
H. Fleischmann
C. Wharton
F. Morse
R. Lovelace

Harvard University
Cambridge, Massachusetts 02138
ATTN: Harvard College Observatory
(Library)
G.S. Vaina
M. Rosenberg

Harvard University
Center for Astrophysics
60 Garden Street
Cambridge, Massachusetts 02138
ATTN: G.B. Field

University of Iowa
Iowa City, Iowa 52240
ATTN: C.K. Goertz
D. Gurnett
G. Knorr
D. Nicholson

University of Houston
Houston, Texas 77004
ATTN: Library

University of Maryland
Physics Dept.
College Park, Maryland 20742
ATTN: K. Papadopoulos
H. Rowland
C. Wu

University of Michigan
Ann Arbor, Michigan 48140
ATTN: E. Fontheim

University of Minnesota
School of Physics
Minneapolis, Minnesota 55455
ATTN: Library
J.R. Winckler
P. Kellogg

M.I.T.
Cambridge, Massachusetts 02139
ATTN: Library
(Physics Dept.):
ATTN: B. Coppi
V. George
G. Bekefi
T. Dupree
R. Davidson
(Elect. Engineering Dept.):
ATTN: R. Parker
A. Bers
L. Smullin
(R.L.E.):
ATTN: Library
(Space Science):
ATTN: Reading Room

Princeton University
Princeton, New Jersey 08540
Attn: Physics Library
Plasma Physics Lab. Library
C. Oberman
F. Perkins
T.K. Chu
H. Okuda
V. Aranasalan
H. Hendel
R. White
R. Kurlsrud
H. Furth
S. Yoshikawa
P. Rutherford

Rice University
Houston, Texas 77001
Attn: Space Science Library
R. Wolf

University of Rochester
Rochester, New York 14627
ATTN: A. Simon

Stanford University
Institute for Plasma Research
Stanford, California 94305
ATTN: Library

Stevens Institute of Technology
Hoboken, New Jersey 07030
ATTN: B. Rosen
G. Schmidt
M. Seidl

University of Texas
Austin, Texas 78712
ATTN: W. Drummond
V. Wong
D. Ross
W. Horton
D. Choi
R. Richardson
G. Leifeste

College of William and Mary
Williamsburg, Virginia 23185
Attn: F. Crownfield

Lawrence Livermore Laboratory
University of California
Livermore, California 94551
ATTN: Library
B. Kruer
J. Thomson
J. Nucholls
J. DeGroot
L. Wood
J. Emmett
B. Lasinsky
B. Langdon
R. Briggs
D. Pearlstein

Los Alamos National Laboratory
P.O. Box 1663
Los Alamos, New Mexico 87545
ATTN: Library
D. Forslund
J. Kindel
B. Bezzerides
H. Dreicer
J. Ingraham
R. Boyer
C. Nielson
E. Lindman
L. Thode

N.O.A.A.
325 Broadway S.
Boulder, Colorado 80302
ATTN: J. Weinstock
Thomas Moore (SEL, R-43)
W. Bernstein
D. Williams

Sandia Laboratories
Albuquerque, New Mexico 87115
ATTN: A. Toepfer
G. Yeonas
D. VanDevender
J. Freeman
T. Wright

Bell Laboratories
Murray Hill, New Jersey 07974
ATTN: A. Hasegawa

Lockheed Research Laboratory
Palo Alto, California 94304
ATTN: M. Walt
J. Cladis
J. Siambis

Physics International Co.
2400 Merced Street
San Leandro, California 94577
ATTN: J. Benford
S. Putnam
S. Stalings
T. Young

Science Applications, Inc.
Lab. of Applied Plasma Studeis
P.O. Box 2351
LaJolla, California 92037
ATTN: L. Linson
J. McBride

NASA/Goddard Space Flight Center
Greenbelt, Maryland 20771
ATTN: M. Goldstein
T. Northrop
T. Birmingham

NASA/Goddard Space Flight Center
Greenbelt, MD 20771
ATTN: A. Figuero Vinas
Code 692

TRW Space and Technology Group
Space Science Dept.
Building R-1, Room 1170
One Space Park
Redondo Beach, California 90278
ATTN: R. Fredericks
W.L. Taylor

National Science Foundation
Atmospheric Research Section (ST)
Washington, D.C. 20550
ATTN: D. Peacock

Goddard Space Flight Center
Code 961
Greenbelt, Maryland 20771
ATTN: Robert F. Benson

NASA Headquarters
Code EE-8
Washington, D.C. 20546
ATTN: Dr. E. Schmerling
Dr. J. Lynch
Dr. D. Butler

Klumpar, David
Center for Space Sciences
P.O. Box 688
University of Texas
Richardson, Texas 75080

Leung, Philip
Dept. of Physics
University of California
405 Hilgard Avenue
Los Angeles, California 90024

Lysak, Robert
School of Physics and Astronomy
University of Minnesota
Minneapolis, MN 55455

Schulz, Michael
Aerospace Corp.
A6/2451, P.O. Box 92957
Los Angeles, California 90009

Shawhan, Stanley
Dept. of Physics & Astronomy
University of Iowa
Iowa City, Iowa 52242

Temerin, Michael
Space Science Lab.
University of California
Berkeley, California 94720

Vlahos, Loukas
Dept. of Physics
University of Maryland
College Park, Maryland 20742

Matthews, David
IPST
University of Maryland
College Park, Maryland 20742

Schunk, Robert W.
Utah State University
Dept. of Physics
Logan, Utah 84322

Director,
Department of Energy
ER20:GTN, High Energy &
Nuclear Physics
Washington, D.C. 20545
ATTN: Dr. Terry Godlove

Director,
Department of Energy
Office of Inertial Fusion
Washington, D.C. 20545
ATTN: Dr. Richard Schriever

Director
Defense Nuclear Agency
Washington, D.C. 20305
ATTN: Dr. Leon Wittwer
Dr. P. Crowley
Dr. Carl Fitz

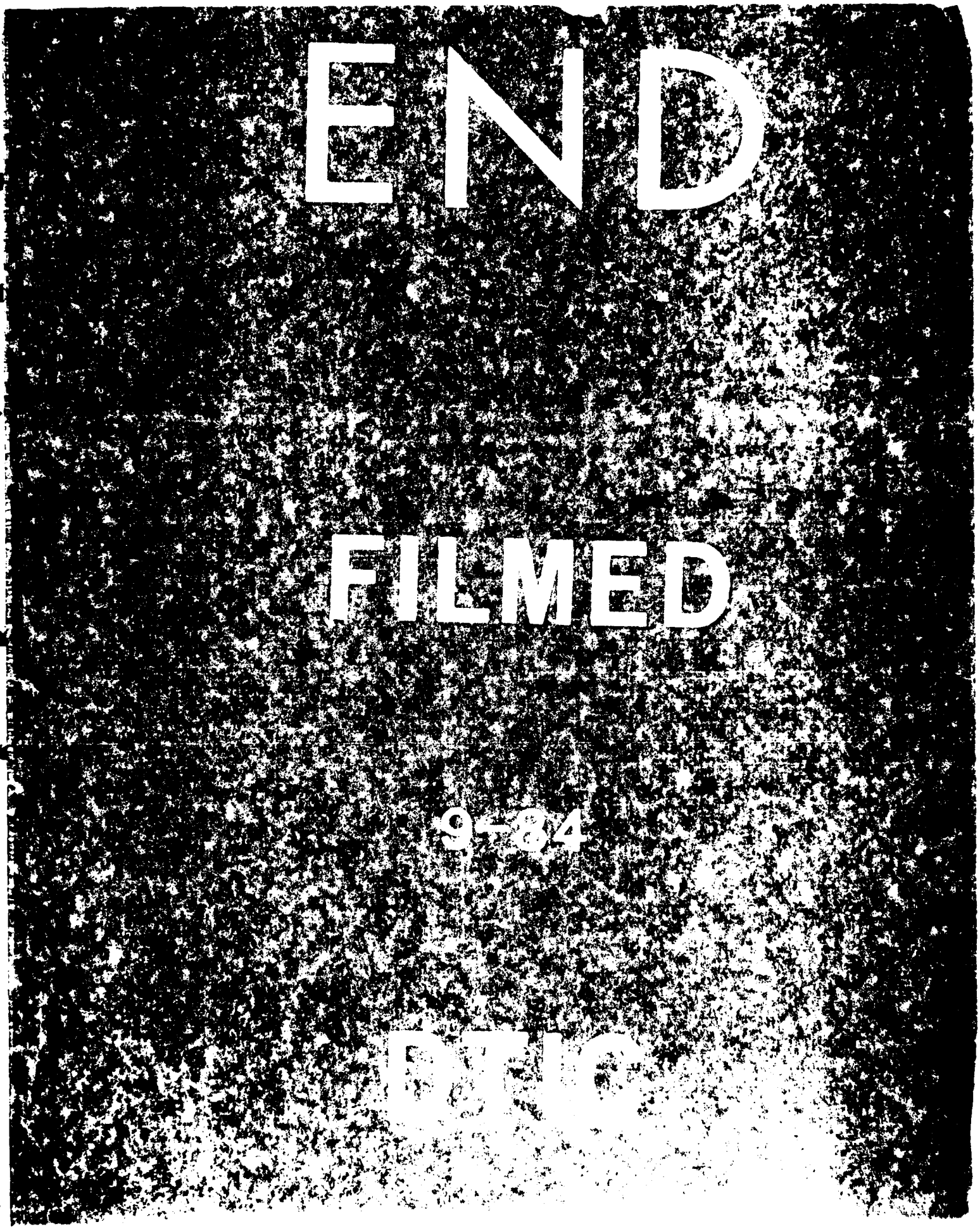
END
FILMED
9-84
DTIC